Dynamical fidelity of a solid-state quantum computation

G. P. Berman,[1] F. Borgonovi,[2,3] G. Celardo,[2,4] F. M. Izrailev,[5] and D. I. Kamenev[1]
[1]*Theoretical Division and CNLS, Los Alamos National Laboratory, Los Alamos, New Mexico 87545*
[2]*Dipartimento di Matematica e Fisica, Università Cattolica, via Musei 41, 25121 Brescia, Italy*
[3]*INFM, Unitá di Brescia and INFN, Sezione di Pavia, Italy*
[4]*INFM, Unità di Milano, Italy*
[5]*Instituto de Física, Universidad Autónoma de Puebla, Apartado Postal J-48, Puebla 72570, Mexico*
(Received 17 June 2002; published 25 November 2002)

In this paper we analyze the dynamics in a spin model of quantum computer. Main attention is paid to the dynamical fidelity (associated with dynamical errors) of an algorithm that allows to create an entangled state for remote qubits. We show that in the regime of selective resonant excitations of qubits there is no danger of quantum chaos. Moreover, in this regime a modified perturbation theory gives an adequate description of the dynamics of the system. Our approach allows us to explicitly describe all peculiarities of the evolution of the system under time-dependent pulses corresponding to a quantum protocol. Specifically, we analyze, both analytically and numerically, how the fidelity decreases in dependence on the model parameters.

DOI: 10.1103/PhysRevE.66.056206 PACS number(s): 05.45.Pq, 05.45.Mt, 03.67.Lx

I. INTRODUCTION

Many suggestions for an experimental realization of quantum computers are related to two-level systems (*qubits*). One of the serious problems in this field is a destructive influence of different kinds of errors that may be dangerous for the stability of quantum computation protocols. In the first line, one should refer to finite temperature effects and interaction of qubits with an environment [1]. However, even in the case when these features can be neglected, errors can be generated by the dynamics itself. This ''dynamical noise'' cannot be avoided since the interaction between qubits and with external fields are both necessary for the implementation of any quantum protocol. However, the interqubit interaction may cause the errors. Therefore, it is important to know to what extent the interaction effects may be dangerous for quantum computation.

As is known from the theory of interacting particles, a two-body interaction between particles may result in the onset of chaos and thermalization, even if the system under consideration consists of a relatively small number of particles (see, for example, the reviews [2–4] and references therein). In application to quantum computers, quantum chaos may play a destructive role since it increases the system sensitivity to external perturbations. Simple estimates obtained for systems of L interacting spins show that with an increase of L the chaos border decreases, and even a small interaction between spins may result in chaotic properties of eigenstates and spectrum statistics. On this ground, it was claimed [5] that quantum chaos for a large number of qubits cannot be avoided, and the idea of a quantum computation meets serious problems.

Recent studies [6] of a realistic 1/2 spin model of a quantum computer show that, in the presence of a magnetic field gradient, the chaos border is independent of L, and that quantum chaos arises in extreme situations only, which are not interesting from the practical viewpoint. One should stress that a nonzero gradient magnetic field is necessary in the model [6] for a selective excitation of different qubits under time-dependent electromagnetic pulses providing a specific quantum protocol.

Another point that should be mentioned in the context of quantum chaos is that typical statements about chaos refer to stationary eigenstates and spectrum statistics. However, quantum computation is essentially a time-dependent problem. Moreover, the time of computation is restricted by the length of a quantum protocol. Therefore, even if stationary Hamiltonians for single pulses reveal chaotic properties, it is still not clear to what extent stationary chaos influences the evolution of a system subjected to a finite number of pulses.

In contrast with our previous studies [6], in this paper we investigate the time evolution of a 1/2 spin quantum computer system subjected to a series of pulses. Specifically, we consider a quantum protocol that allows to create an entangled state for remote qubits. For this, we explore the model in the so-called *selective* regime, using both analytical and numerical approaches. Our analytical treatment shows that in this regime there is no fingerprint of quantum chaos. Moreover, we show that a kind of perturbative approach provides a complete description of the evolution of our system.

We concentrate our efforts on the introduced quantity (*dynamical fidelity*). This quantity characterizes the performance of quantum computation associated with the *dynamical* errors. Dynamical fidelity differs from the fidelity that is widely used nowadays in different applications to quantum computation and quantum chaos, see, for instance, Ref. [7], because we do not add any random variation in the Hamiltonian. Our study demonstrates an excellent agreement of analytical predictions with numerical data.

The structure of the paper is as follows. In Sec. II we discuss our model and specify the region of parameters for which our study is performed. In Sec. III we explore the possibility of quantum chaos in the selective regime, and analytically show that chaos cannot occur in this case. We provide all details concerning the quantum protocol in Sec. IV, and demonstrate how perturbation theory can be applied to obtain an adequate description of the fidelity in dependence on the system parameters. Here, we also present nu-

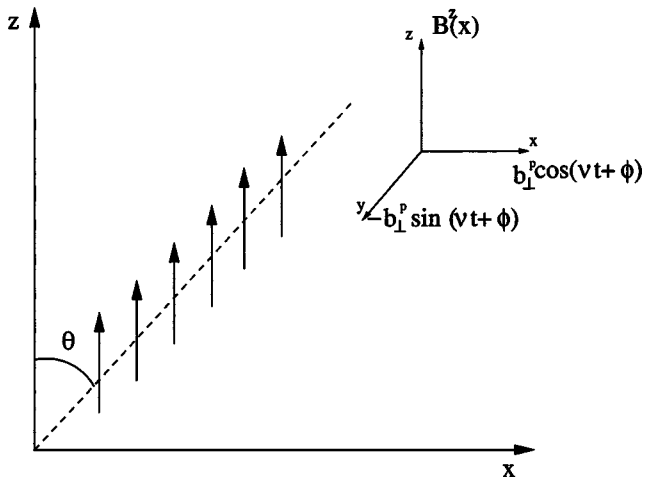

FIG. 1. Spin model for quantum computation. Also indicated is the direction of the magnetic field (1).

merical data and compare them with the predictions based on the perturbative approach. Section V summarizes our results.

II. SPIN MODEL OF A QUANTUM COMPUTER

Our model is represented by a one-dimensional chain of L identical 1/2 spins placed in an external magnetic field, see Fig. 1.

It was first proposed in Ref. [8] (see also Refs. [9–11]) as a simple model for solid-state quantum computation. Some physical constraints are necessary in order to let it operate in a quantum computation regime. To provide a selective resonant excitation of spins, we assume that the time independent part $B^z = B^z(x)$ of the magnetic field is nonuniform along the spin chain. The nonzero gradient of the magnetic field provides different Larmor frequencies for different spins. The angle θ between the direction of the chain and the z axis satisfies the condition, $\cos\theta = 1/\sqrt{3}$. In this case the dipole-dipole interaction is suppressed, and the main interaction between nuclear spins is due to the Isinglike interaction mediated by the chemical bonds, as in a liquid state nuclear magnetic resonance (NMR) quantum computation [1].

In order to realize quantum gates and implement operations, it is necessary to apply selective pulses to single spins. The latter can be distinguished, for instance, by imposing a constant-gradient magnetic field that results in the Larmor frequencies $\omega_k = \gamma B^z(x_k) \equiv \omega_0 + ak$, where γ is the spin gyromagnetic ratio and x_k is the position of the kth spin. If the distance between the neighboring nuclear spins is $\Delta x = 0.2$ nm, and the frequency difference between them is $\Delta f = a/2\pi = 1$ kHz, then the corresponding gradient of the magnetic field can be estimated as follows, $|dB^z/dx| = \Delta f/(\gamma/2\pi)\Delta x \approx 1.2\times 10^4$ T/m. Here we used the gyromagnetic ratio for a proton, $\gamma/2\pi \approx 4.3\times 10^7$ Hz/T. Such a magnetic field gradient is experimentally achievable, see, for example, Refs. [12,13].

In our model the spin chain is also subjected to a transversal circular polarized magnetic field. Thus, the expression for the total magnetic field has the form [6,10,11],

$$\vec{B}(t) = [b_\perp^p \cos(\nu_p t + \varphi_p), -b_\perp^p \sin(\nu_p t + \varphi_p), B^z(x)]. \quad (1)$$

As mentioned above, here $B^z(x)$ is the constant magnetic field oriented in the positive z direction, with a positive x gradient (therefore, $a>0$ in the expression for the Larmor frequencies). In the above expression, $b_\perp^p$, ν_p, and φ_p are the amplitudes, frequencies, and phases of a circular polarized magnetic field, respectively. The latter is given by the sum of $p=1,\ldots,P$ rectangular time-dependent pulses of length $t_{p+1}-t_p$, rotating in the (x,y)-plane and providing a quantum computer protocol.

Thus, the quantum Hamiltonian of our system has the form

$$\mathcal{H} = -\sum_{k=0}^{L-1}\left[\omega_k I_k^z + 2\sum_{n>k} J_{k,n} I_k^z I_n^z\right] - \frac{1}{2}\sum_{p=1}^{P}\Theta_p(t)\Omega_p \sum_{k=0}^{L-1}(e^{-i\nu_p t - i\varphi_p} I_k^- + e^{i\nu_p t + i\varphi_p} I_k^+), \quad (2)$$

where the "pulse function" $\Theta_p(t)$ equals 1 only during the pth pulse, for $t_p < t \leq t_{p+1}$, otherwise it is zero. The quantities $J_{k,n}$ stand for the Ising interaction between two qubits, ω_k are the frequencies of spin precession in the B^z magnetic field, Ω_p is the Rabi frequency of the pth pulse, $I_k^{x,y,z} = (1/2)\sigma_k^{x,y,z}$ with $\sigma_k^{x,y,z}$ as the Pauli matrices, and $I_k^\pm = I_k^x \pm i I_k^y$.

For a specific pth pulse, it is convenient to represent the Hamiltonian (2) in the coordinate system that rotates with the frequency ν_p. Therefore, for the time $t_p < t \leq t_{p+1}$ of the pth pulse our model can be reduced to the *stationary* Hamiltonian

$$\mathcal{H}^{(p)} = -\sum_{k=0}^{L-1}(\xi_k I_k^z + \alpha I_k^x - \beta I_k^y) - 2\sum_{n>k} J_{k,n} I_k^z I_n^z, \quad (3)$$

where $\xi_k = (\omega_k - \nu_p)$, $\alpha = \Omega_p \cos\varphi_p$, and $\beta = \Omega_p \sin\varphi_p$.

We start our considerations with the simplified case of the Hamiltonian (3) for a single pulse, by choosing $\varphi_p = 0$. We also assume a constant interaction between nearest neighbors qubits only ($J_{k,n} = J\delta_{k,k+1}$), and we put $\Omega_p = \Omega$. Then the Hamiltonian (3) takes the form

$$\mathcal{H}^{(p)} = -\sum_{k=0}^{L-1}\xi_k I_k^z - 2J\sum_{k=0}^{L-2} I_k^z I_{k+1}^z - \Omega\sum_{k=0}^{L-1} I_k^x \equiv H_0 + V. \quad (4)$$

In z representation the Hamiltonian matrix of size 2^L is diagonal for $\Omega = 0$. For $\Omega \neq 0$, nonzero off-diagonal matrix elements are simply $H_{kn} = H_{nk} = -\Omega/2$ with $n \neq k$. The matrix is very sparse, and it has a specific structure in the basis reordered according to an increase of the number s. The latter is written in the binary representation, $s = i_{L-1}, i_{L-2}, \ldots, i_0$ (with $i_s = 0$ or 1, depending on whether the single-particle state of the ith qubit is the ground state or

the excited one). The parameter Ω thus is responsible for a nondiagonal coupling, and we hereafter define it as a "perturbation."

In our previous studies [6] we have analyzed the so-called *nonselective* regime that is defined by the conditions, $\Omega \gg \delta\omega_k \gg J$. This inequality provides the simplest way to prepare a homogeneous superposition of 2^L states needed for the implementation of both Shor and Grover algorithms. Our analytical and numerical treatment of the model (2) in this regime has shown that a constant gradient magnetic field (with nonzero value of a) strongly reduces the effects of quantum chaos. Namely, the chaos border turns out to be independent on the number L of qubits. As a result, for nonselective excitation quantum chaos can be practically neglected (see details in Ref. [6]).

Below we consider another important regime called *selective excitation*. In this regime each pulse acts selectively on a chosen qubit, resulting in a resonant transition. During the quantum protocol, many such resonant transitions take place for different p pulses, with different values of $\nu_p = \omega_k$. The region of parameters for the selective excitation is specified by the following conditions [10]:

$$\Omega \ll J \ll a \ll \omega_k . \tag{5}$$

The meaning of these conditions will be discussed in next sections.

III. ABSENCE OF QUANTUM CHAOS IN THE SELECTIVE EXCITATION REGIME

Here, we consider the properties of the stationary Hamiltonian (4) in the regime of selective excitation. In order to estimate the critical value of the interaction J, above which one can expect random properties of eigenstates, one needs to compare the typical value of the off-diagonal matrix elements $(\Omega/2)$ with the mean energy spacing δ_f for unperturbed many-body states that are directly coupled by these matrix elements. Therefore, the condition for the onset of chaos has the form

$$\frac{\Omega}{2} > \delta_f \approx \frac{(\Delta E)_f}{M_f}. \tag{6}$$

Here $(\Delta E)_f$ is the maximal difference between the energies $E_0^{(2)}$ and $E_0^{(1)}$ corresponding to a specific many-body state $|1\rangle$, and all other states $|2\rangle$ of H_0, that have nonzero couplings $\langle 1|V|2\rangle$. Correspondingly, M_f is the number of many-body states $|2\rangle$ coupled by V to the state $|1\rangle$. A further average over all states $|1\rangle$ should be then performed.

In fact, such a comparison (6) is just the perturbation theory in the case of two-body interaction. Strictly speaking, the above condition in a strong sense $(\Omega \gg \delta_f)$ means that exact eigenstates consist of many unperturbed $(V=0)$ states. Typically, the components of such compound states can be treated as uncorrelated entries, thus resulting in a random structure of excited many-body states. However, one should note that in specific cases when the total Hamiltonian is integrable (or quasi-integrable), the components of excited states have strong correlations and cannot be considered as random, although the number of components with large amplitudes can be extremely large (see details in Ref. [6]).

It is relatively easy to estimate M_f in the regime of selective excitation. Let us consider an eigenstate of H_0, $|1,0,0,0,1,0,\ldots,0,0,1,0\rangle$, as a collection of 0's and 1's that correspond to $-1/2$ and $1/2$ spin values. Since the perturbation V is a sum of L terms, each of them flipping one single spin, one gets $M_f = L$.

In order to estimate $(\Delta E)_f$, let us first consider the action of V on the kth spin, and for each spin compute the relative energy difference between the final and the initial energy. One can find that if the kth spin has the value 1/2, there are four possible configurations of neighbor spins coupled by the perturbation

$$\begin{aligned} &|\ldots 0,1,0\ldots\rangle \rightarrow |\ldots 0,0,0\ldots\rangle, \\ &|\ldots 1,1,1\ldots\rangle \rightarrow |\ldots 1,0,1\ldots\rangle, \\ &|\ldots 1,1,0\ldots\rangle \rightarrow |\ldots 1,0,0\ldots\rangle, \\ &|\ldots 0,1,1\ldots\rangle \rightarrow |\ldots 0,0,1\ldots\rangle. \end{aligned} \tag{7}$$

If the kth spin has the value $-1/2$, there are also four possible different arrangements,

$$\begin{aligned} &|\ldots 0,0,0\ldots\rangle \rightarrow |\ldots 0,1,0\ldots\rangle, \\ &|\ldots 1,0,1\ldots\rangle \rightarrow |\ldots 1,1,1\ldots\rangle, \\ &|\ldots 1,0,0\ldots\rangle \rightarrow |\ldots 1,1,0\ldots\rangle, \\ &|\ldots 0,0,1\ldots\rangle \rightarrow |\ldots 0,1,1\ldots\rangle, \end{aligned} \tag{8}$$

which are the inverse transitions of Eq. (7). Correspondingly, the energy changes are determined by the relation,

$$|E_0^{(f)} - E_0^{(i)}| = |\xi_k \pm 2J|, |\xi_k|, \quad k = 1,\ldots,L-2. \tag{9}$$

The analysis for the border spins can be performed in a similar way, and one gets four possible configurations, with the following energy changes:

$$|E_0^{(f)} - E_0^{(i)}| = |\xi_k \pm J|, \quad k = 0, L-1. \tag{10}$$

Summarizing the above findings, and setting, for instance, $\nu_p = \omega_0$, one can conclude that $(\Delta E)_f$ can be estimated as follows:

$$(\Delta E)_f = \mathrm{Max}(|E_0^{(f)} - E_0^{(i)}|) = \omega_{L-1} - \omega_0 + J. \tag{11}$$

As a result, the condition for the onset of quantum chaos can be written in the form

$$\frac{\Omega}{2} > \frac{(\Delta E)_f}{M_f} = \frac{\omega_{L-1} - \omega_0 + J}{L} = \frac{a(L-1) + J}{L} \tag{12}$$

or

$$\Omega > \Omega_{cr} \simeq 2a + \frac{2J}{L}. \tag{13}$$

However, this critical value is outside the range of parameters required to be in the selective excitation regime $\Omega < a$

[see inequality (6)]. Thus, we can conclude that quantum chaos for stationary states cannot appear in the selective excitation regime. Note that the analysis is done for a single pulse of a time-dependent perturbation.

IV. FIDELITY OF A QUANTUM PROTOCOL

The analytical results obtained above, show that, during a single electromagnetic pulse, the system can be described by perturbation theory. Indeed, if the matrix elements of perturbation are smaller than the energy spacing between directly coupled many-body states, exact eigenstates can be obtained by perturbation theory. Thus, one can expect that for a series of time-dependent pulses the system evolution can also be treated making use of a perturbative approach.

In what follows, we study the system dynamics by applying a specific set of pulses (quantum protocol) in order to create an entangled state for remote qubits (with $k=0$ and $k=L-1$) starting from the ground state, $|\psi_0\rangle = |0_{L-1},\ldots,0_1,0_0\rangle$ (we omit the subscripts below). Our main interest is in estimating the errors that appear due to unwanted excitations of qubits. We show that these errors can be well understood and estimated on the basis of the perturbation theory developed for our time-dependent Hamiltonian (2), in the parameter range where the protocol holds.

A. Selective excitation regime and perturbation theory

Any protocol is a sequence of unitary transformations applied to some initial state in order to obtain a final ideal state $|\psi^i\rangle$. In this model of quantum computer the protocol is realized by applying a number of specific rf pulses, so that we get a state $|\psi^r\rangle$ which is, in principle, different from the ideal state $|\psi^i\rangle$. The difference between the real state $|\psi^r\rangle$ and the ideal state $|\psi^i\rangle$ can be characterized by a *dynamical fidelity*,

$$F=|\langle\psi^i|\psi^r\rangle|^2. \tag{14}$$

Note that, in our case, the dynamical fidelity F does not explicitly depend on a perturbation parameter added in the Hamiltonian (2) in order to get a distorted evolution, as is typically assumed in the study of quantum chaos. Indeed, the real final state is determined by the total Hamiltonian (2),

$$|\psi^r\rangle=\hat{U}(T)|\psi_0\rangle\equiv\prod_{p=1}^{P}\hat{T}\exp\left(-i\int_{t_{p-1}}^{t_p}H(t)dt\right)|\psi_0\rangle, \tag{15}$$

where $T=t_p$ is the total time to entangle spins, $\hat{U}(T)$ is the unitary operator given by the sequence of pulses in the protocol, and $\hat{T}$ is the usual time-ordered product. Therefore, it is not possible to identify a single perturbation parameter that is responsible for a ''wrong'' evolution of the system.

The selective excitation regime is characterized by the action of pulses that are resonant with a transition between two energy states which differ for the state (up or down) of one spin only. A close inspection of the time independent Hamiltonian (4), defines the region of parameters where the selective excitation of single spins can be performed.

Diagonal elements of Hamiltonian (4) are given by the eigenvalues $E_0^{(i)}$ of H_0, while nonzero off-diagonal elements are constant and equal to $-\Omega/2$. In order to have a resonant transition between two energy states, their energy difference Δ has to be zero. However, for each state no more than one resonant transition should be allowed. So, we require the energy differences given by Eqs. (9) and (10) to be different from zero, apart from the wanted transition. This leads to the following set of equalities (''fake transitions''):

$$\begin{aligned} J&=a\frac{k}{4} \quad \text{when} \quad k=1,\ldots,L-3,\\ J&=a\frac{k}{2} \quad \text{when} \quad k=1,\ldots,L-3,\\ J&=ak \quad \text{when} \quad k=1,\ldots,L-2,\\ J&=a\frac{k}{3} \quad \text{when} \quad k=1,\ldots,L-2. \end{aligned} \tag{16}$$

From Eqs. (16) it is easy to see that the first ''fake'' transition appears for $J_1=a/4$, the second for $J_2=a/2$, and so on up to the last one for $J_f=a(L-2)$. All these resonances can be avoided if we choose $a\gg 4J$ (due to the resonance finite width the condition $a>4J$ is not sufficient).

Transitions can be defined according to their energy difference Δ, (1) *resonant transitions*, $\Delta=0$; (2) *near-resonant transitions*, $\Delta\sim J$; (3) *non-resonant transitions*, $\Delta\sim a$.

For $a\gg 4J$, each state can undergo one resonant or near-resonant transition only, and many nonresonant ones. The latter can be neglected if we choose $a\gg\Omega$. Under these conditions we can form couples of states, connected by resonant or near-resonant transitions, and we can rearrange the Hamiltonian matrix (4) by 2×2 block matrices representing all resonant and near-resonant transitions. In this way the dynamical evolution of the system can be described as a two-state problem.

Using this procedure, the entire sequence of pulses can be evaluated. Note that special attention has to be paid to an additional phase shift that arises between any two pulses, due to the change of frame. We remind that the transformation between the rotating and the laboratory frame is given by the expression

$$|\psi(t)\rangle_{Lab}=\exp\left(i\nu_p t\sum_k I_k^z\right)|\psi(t)\rangle_{Rot}. \tag{17}$$

Indeed, let us consider an initial basis state $|m\rangle$ at time $t=0$, and find the probability for a resonant ($\Delta=0$) or near-resonant ($\Delta\sim J$) transition to the state $|p\rangle$ with the energy difference E_p-E_m. Here E_p and E_m are the eigenenergies of the time-independent part of the Hamiltonian (2), written in the laboratory frame.

Setting

$$\psi(t)=\sum_n c_n(t)|n\rangle, \tag{18}$$

and $c_p(0)=0$, after the application of a pulse for a time τ one gets, in the laboratory frame,

$$c_m(\tau)=c_m(0)\left[\cos\left(\frac{\lambda\tau}{2}\right)+i\frac{\Delta}{\lambda}\sin\left(\frac{\lambda\tau}{2}\right)\right]e^{-i(\Delta\tau/2)-iE_m\tau},$$

$$c_p(\tau)=c_m(0)\left[i\frac{\Omega}{\lambda}\sin\left(\frac{\lambda\tau}{2}\right)\right]e^{i(\Delta\tau/2)-iE_p\tau}, \tag{19}$$

where $\lambda=\sqrt{\Omega^2+\Delta^2}$.

As we can see, the parameter ϵ determined as

$$\epsilon=\frac{\Omega^2}{\Omega^2+\Delta^2}\sin^2\left(\frac{\tau}{2}\sqrt{\Omega^2+\Delta^2}\right) \tag{20}$$

characterizes the probability of resonant and near-resonant transitions. In particular, the probability of unwanted near-resonant transitions goes like ϵ, and it can be reduced by assuming $J\gg\Omega$. Combining all the above expression, we get the condition (5).

Correspondingly, the probability for a nonresonant transition (neglecting terms of the order $1/L$, and assuming $a\gg\Omega$) is given by the parameter η [11],

$$\eta=\frac{\Omega^2}{4a^2}. \tag{21}$$

We would like to stress that even if the ideal state has been constructed taking into account resonant transitions only, our dynamical fidelity is a measure of dynamical errors that are due to near-resonant and nonresonant transitions.

Let us now briefly discuss the perturbative approach that is based on recent studies published in Ref. [11]. The main idea is that for each pth pulse the unperturbed basis can be rearranged in such a way that the Hamiltonian matrix is represented by 2×2 block matrices, as described above. This is what we call *unperturbed* Hamiltonian for a specific pth pulse. One should note that this *unperturbed* Hamiltonian is Ω dependent. Let us now define by $\mathcal{V}$ the Ω dependent part that is responsible for nonresonant transition and not described by the 2×2 block matrices. Then it is easy to obtain the unperturbed eigenstates, $|\psi_q^0\rangle$, and the unperturbed eigenvalues, ϵ_q^0, by diagonalizing each of the 2×2 blocks independently.

After this step, one can compute the *perturbed* eigenstates by taking into account the first-order terms only,

$$|\psi_q\rangle=|\psi_q^0\rangle+\sum_{q'\neq q}\frac{\langle\psi_q^0|\mathcal{V}|\psi_{q'}^0\rangle}{\epsilon_q^0-\epsilon_{q'}^0}|\psi_{q'}^0\rangle. \tag{22}$$

Note that this perturbative approach is supposed to be valid when Eqs. (16) are not satisfied, and when the errors due to near-resonant transitions are much larger than the errors due to nonresonant ones, $\epsilon\gg\eta$.

B. Quantum protocol

Let us briefly sketch the algorithm and the particular protocol that was developed in Ref. [10]. Starting from the ground state $|\psi_0\rangle=|0\ldots0\rangle$ and applying a number of specific pulses, we would like to generate the following entangled state:

$$|\psi^i\rangle=\frac{1}{\sqrt{2}}(|0\ldots0\rangle+|10\ldots.01\rangle). \tag{23}$$

This algorithm could serve, for instance, as the first step for a more general teleportation protocol, and for an implementation of conditional quantum logic operations.

The algorithm can be realized in the following way (for details see Ref. [10]):

$$\begin{aligned}|0,\ldots,0\rangle&\rightarrow(|0,\ldots,0\rangle+|1,0,\ldots,0\rangle)\\&\rightarrow(|0,\ldots,0\rangle+|1,1,0,\ldots,0\rangle)\\&\rightarrow(|0,\ldots,0\rangle+|1,1,1,0,\ldots,0\rangle)\\&\rightarrow(|0,\ldots,0\rangle+|1,0,1,0,\ldots,0\rangle)\\&\rightarrow\ldots\rightarrow(|0,\ldots,0\rangle+|1,0,\ldots,1\rangle).\end{aligned} \tag{24}$$

Physically, the above algorithm can be done by applying suitable rf pulses that are resonant to the desired transitions. The latter are originated from induced Rabi oscillations between the resonant states.

To flip the kth spin we have to choose the frequency ν of the rf pulse according to the relation $\nu_p=E_1-E_2$, where $|1\rangle$, $|2\rangle$ are the states involved in the transition and E_1, E_2 are the eigenenergies of the time-independent part of Hamiltonian (2). For instance, for the first pulse we put, $\nu_1=|E_{|1,0,\ldots,0\rangle}-E_{|0,\ldots,0\rangle}|$, and we have to apply it for a time $t_1=\pi/2\Omega$ to get equal superposition of the states involved in the transition. For other pulses we require that the first state $(|0,\ldots,0\rangle)$ remains the same (apart from an additional phase), while the second state flips the kth spin. In other words, the probability of unwanted states is due to nonresonant transitions of both states of the right-hand side of Eq. (24), and to near-resonant ones of the first state only. Specifically, the state $|0,\ldots,0\rangle$ undergoes near-resonant transitions with $\Delta=2J$ for each pulse, except the first one which is resonant, and the fourth for which $\Delta=4J$. Also, at each pulse the state $|0,\ldots,0\rangle$ get an additional phase, see Eqs. (19). We took them into account in the definition of the ideal state, see details in Sec. IV C.

Since in the selective excitation regime we have $\epsilon\gg\eta$, contributions from near-resonant transitions are much larger than the ones due to nonresonant transitions. Our algorithm consists of $2L-2$ separate pulses, therefore, some modifications are necessary in order to be able to control small unwanted probability. For the product of probabilities this implies $2L\epsilon<1$ and $2L\eta<1$, or

$$\frac{\Omega}{J}\ll\sqrt{\frac{2}{L}},\quad\frac{\Omega}{a}\ll\sqrt{\frac{2}{L}} \tag{25}$$

for $L\gg1$.

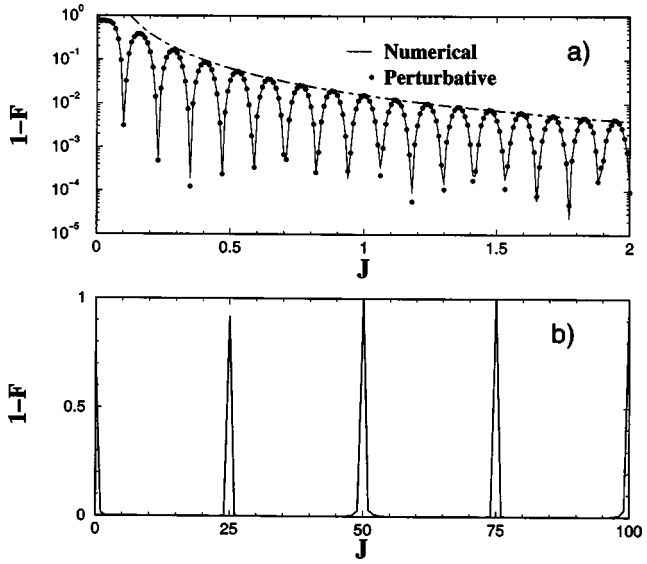

FIG. 2. The dependence $1-F$ is shown as a function of the Ising coupling J for $L=6$ spins, $\Omega=0.118$, and $a=100$. Full line represents the numerical data for the dynamical fidelity F defined by Eq. (14), and obtained from direct numerical computation of the system evolution. (a) Full circles stand for perturbative calculations, and full curve corresponds to numerical results. (b) The same numerical results as in (a), but for a larger range of J. The theoretical expression as given by Eq. (32) is also shown in (a).

Before discussing our numerical results we would like to stress that in contrast to what is mainly considered in the literature, the time for our dynamical fidelity is not an independent variable. Indeed, the length of the protocol is determined by the total number of qubits, L. Specifically, $2L-2$ pulses are necessary in order to create the entangled state, so that the protocol time T is proportional to the number of qubits.

C. Dynamical fidelity: Theory and numerical data

Quite unexpectedly, the dynamical fidelity (14) increases with an increase of the Ising coupling J, as soon as $J \ll a/4$. Indeed, the probability of unwanted near-resonant transitions is proportional to $\epsilon \sim (\Omega/J)^2$ [see Eq. (20), where $\Delta \sim J$ for near-resonant transitions]. Therefore, the larger is J, the smaller is the probability of near-resonant transitions, and the larger is the dynamical fidelity F.

In Fig. 2 we show how the dynamical fidelity (14) depends on the interqubit interaction J. For convenience, the function $1-F$ is shown here and below, instead of F. Numerical data have been obtained in two different ways. Full curve corresponds to exact computation of the time-dependent Hamiltonian (2). Data in Fig. 2(a) are compared with those obtained from the perturbative approach explained above.

Apart from very strong peaks [see Fig. 2(b)] for which the dynamical fidelity vanishes, one can say that the global tendency is an improvement of the dynamical fidelity for larger values of J. However, strong oscillations occur reflecting a resonant nature of the dynamics of our system. Perfect agreement between perturbative results and numerical data is found for very large variations of the interaction strength J.

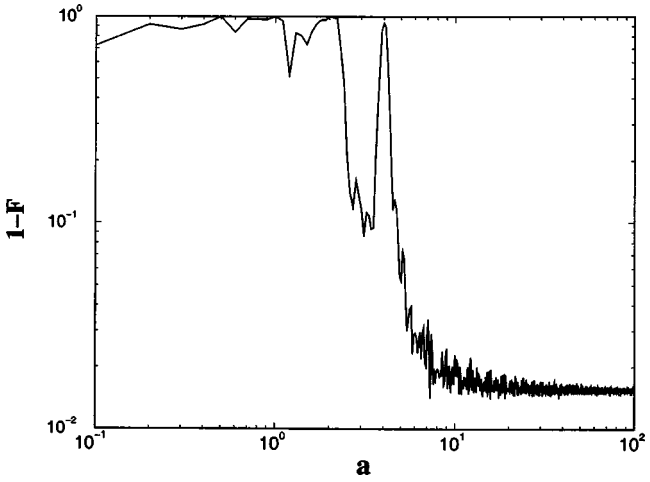

FIG. 3. The dependence $1-F$ as a function of the gradient of a magnetic field is shown for $L=6$ spins, $\Omega=0.118$, and $J=1$. As one can see, for $a<4J$ the fidelity is not as good as for $a>4J$.

High peaks for $1-F$, clearly seen in Fig. 2(b), occur for those J values given by Eqs. (16), where quantum algorithm fails. Thus, one should avoid these situations in a quantum computation.

As for the minima in Fig. 2(a) for which the dynamical fidelity is close to one, they occur when $\epsilon=0$, or, when

$$J=\frac{\Omega}{2}\sqrt{4k^2-1},$$

where k is an integer number. This relation corresponds to the $2\pi k$ condition [10,11,14].

Let us now explore the dependence of the dynamical fidelity on the parameter a which is proportional to the gradient of the external magnetic field, $a=\gamma\Delta x[dB^z(x)/dx]$, where Δx is the distance between neighboring qubits (below, we shall refer to the parameter a as the magnetic field gradient). Numerical data for the dependence of $1-F$ on a are presented in Fig. 3. One can see that the dynamical fidelity is getting better for large enough values of a. We already mentioned that for $a<4J$ a problem may arise in the protocol due to ''fake'' transitions. On the other side, in the regime $a \gg 4J$ the dynamical fidelity reaches an asymptotic value that depends on J and Ω only, see Fig. 3.

It is also important to understand the dependence of the dynamical fidelity on the Rabi frequency Ω. The data manifest two specific properties demonstrated in Fig. 4. The first one is a global decrease of the dynamical fidelity with an increase of Ω. The second peculiarity is due to strong oscillations that occur for $\epsilon=0$, namely, for those Ω values corresponding to the $2\pi k$ conditions,

$$\Omega_k=\frac{2J}{\sqrt{4k^2-1}}. \tag{26}$$

For these Ω_k values, near-resonant transitions vanish, and nonresonant transitions remain only. Thus, the dynamical fi-

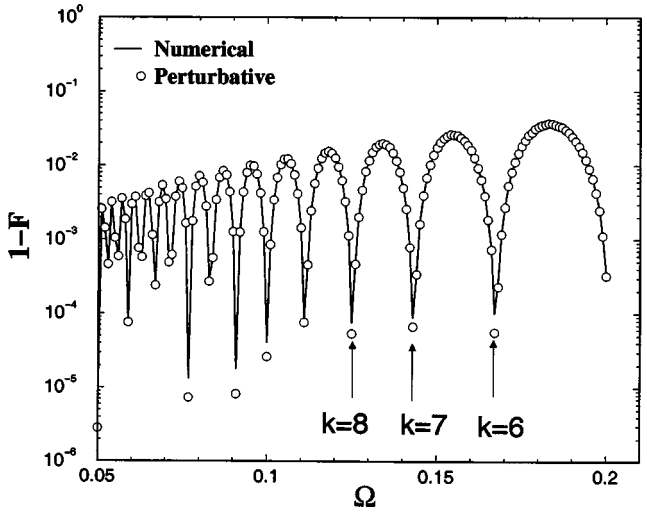

FIG. 4. The difference $1-F$ as a function of the Rabi frequency Ω for $L=6$ spins, $J=1$, and $a=100$. Full curve is the result of direct numerical simulation, circles are obtained from the perturbative approach described in the text. Arrows show few resonant values of Ω given by Eq. (26).

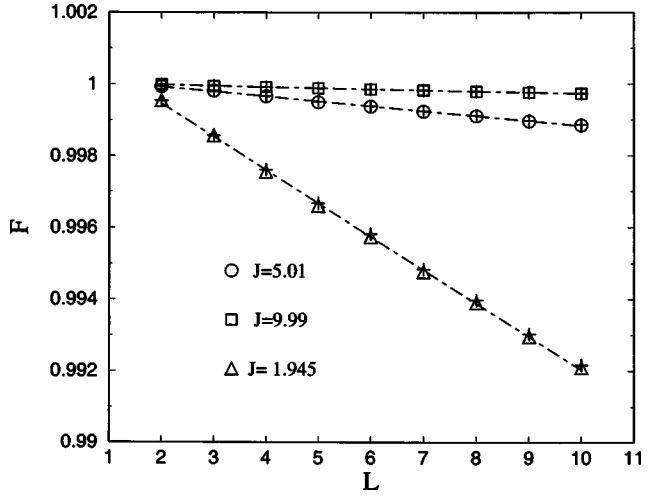

FIG. 5. The dynamical fidelity as a function of the number L of spins, for different J values and $\Omega=0.118$, $a=100$. Numerical data (triangles for $J=1.945$, circles for $J=5.01$, and squares for $J=9.99$) are compared with the results from the perturbation theory (crosses). Also shown are the best linear fits (dot-dashed lines).

delity has maxima that provides, in principle, the best condition for a quantum computation.

Nevertheless, let us consider the values of Ω that correspond to maxima in Fig. 4. This we do in order to make an estimate in the worst possible condition for quantum computation. A brief analysis of the fidelity for the specific values $\Omega=\Omega_k$ will be sketched in the last subsection. As one can see, for values of Ω different from Ω_k, the ''average'' dynamical fidelity increases when the Rabi frequency decreases. This is due to the fact that the probability to generate unwanted states (due to both nonresonant and near-resonant transitions), is proportional to $(\Omega/\Delta)^2$. Therefore, the smaller Ω is, the more reliable is the algorithm. Note that the agreement with the perturbative approach is excellent.

However, we cannot choose an extremely small value of Ω since it implies a large time duration of the pulse ($\tau \sim \pi/\Omega$). Note that the total time for a quantum protocol should be kept well below the decoherence time (the latter can be quite large for nuclear spins [15]). Taking that into account, an optimal choice is to choose the largest possible value, $\Omega=\Omega_2=2J/\sqrt{15}<J$, and large enough value of a (in order to significantly suppress the nonresonant transitions).

D. Fidelity: Dependence on the number of qubits

Finally, we studied the dependence of the dynamical fidelity on the number L of spins in the chain. As was noted before, for a chosen protocol its length is proportional to L. Numerical data clearly manifest a linear decrease of the dynamical fidelity with the number of qubits, see Fig. 5.

Let us give now a brief analytical derivation of the dependence of fidelity on the number of qubits.

Given the real and the ideal final state,

$$|\psi^r\rangle=\sum_k c_k^r|\psi_k\rangle, \quad |\psi^i\rangle=c_0^i|0\ldots0\rangle+c_1^i|10\ldots01\rangle$$

and using Eq. (14), we have

$$F=|c_0^{i*}c_0^r+c_1^{i*}c_1^r|^2. \tag{27}$$

In Eq. (27) the ideal coefficients are given by

$$c_0^i=\frac{1}{\sqrt{2}}e^{i\theta_0^i}=\frac{1}{\sqrt{2}}e^{-iE_0T},$$

$$c_1^i=\frac{1}{\sqrt{2}}e^{i\theta_1^i}=\frac{1}{\sqrt{2}}i^P\exp\left(-i\sum_{p=1}^{P}E_p(t_{p+1}-t_p)\right), \tag{28}$$

where T is the total protocol time and $P=2L-2$ is the number of pulses, E_0 and E_p are the eigenenergies of the time-independent part of Hamiltonian (2). Specifically, E_p are the eigenenergies of the intermediate states, as given by Eq. (24), and $t_{p+1}-t_p$ is the duration of the p pulse [$t_{p+1}-t_p=\pi/(2\Omega)$ if $p=1$ and $t_{p+1}-t_p=\pi/\Omega$ if $p\neq1$].

In the same way, we define

$$c_0^r=\rho_0e^{i\theta_0^r}, \quad c_1^r=\rho_1e^{i\theta_1^r},$$

with the above definitions the fidelity becomes

$$F=\frac{1}{2}[\rho_0^2+\rho_1^2+2\rho_0\rho_1\cos(\Delta\theta_0-\Delta\theta_1)], \tag{29}$$

where $\Delta\theta_0=\theta_0^r-\theta_0^i$, and $\Delta\theta_1=\theta_1^r-\theta_1^i$.

The ideal state is defined by resonant transitions only, as explained in Sec. IV A, and Eqs. (28) are easily obtained from Eqs. (19).

On the other side, the real state differs from the ideal one because of the errors due to nonresonant and near-resonant transitions. In particular, the coefficient c_1^r differs from the coefficient c_1^i because of errors due to non-resonant transi-

tions only, while c_0^r differs from c_0^i because of errors due to both nonresonant and near-resonant transitions.

Since we neglect nonresonant transitions ($\eta \ll 1$) we can put $c_1^r = c_1^i$.

Differently, near-resonant transitions will act on c_0^r only, giving a change in both its modulus and phase.

The change of phase α, in one pulse, for a near-resonant transition, can be obtained from Eqs. (19),

$$\alpha = \arctan\left[\frac{\Delta}{\lambda}\tan\left(\frac{\lambda\tau}{2}\right)\right] - \frac{\Delta\tau}{2},$$

therefore, for $2L-3$ pulses (since during the first pulse no near-resonant transitions occur), we have

$$\Delta\theta_0 = (2L-3)\alpha. \tag{30}$$

Accordingly, we can define in a different way the ideal state, changing the phase of $c_0^i \to c_0^i \exp[i(2L-3)\alpha]$, in order to have $\Delta\theta_0 = 0$.

Let us notice that any phase shift between the states $|0\ldots.0\rangle$ and $|10\ldots.01\rangle$ can be eliminated by applying two additional pulses.

From Eqs. (19) we can also evaluate the error on the modulus of the coefficient c_0^r. The probability for the state $|0\ldots0\rangle$ to make a transition to an unwanted state is determined by the parameter ϵ, see Eq. (20). In this way, at the end of the protocol, we have $|c_0^r|^2 = \frac{1}{2}(1-\epsilon)^{(2L-3)}$.

Assuming $(2L-3)\epsilon \ll 1$, we can write

$$\rho_0 \sim \frac{1}{\sqrt{2}}\left[1-(2L-3)\frac{\epsilon}{2}\right].$$

In this way Eq. (29) becomes

$$F \sim 1-(2L-3)\frac{\epsilon}{2}. \tag{31}$$

Since $\epsilon \sim \Omega^2/4J^2$, we get

$$F \sim \left(1+\frac{3\Omega^2}{8J^2}\right) - \left(\frac{\Omega^2}{4J^2}\right)L, \tag{32}$$

which implies a linear decrease of the dynamical fidelity with an increase of the number of qubits, L. The slope is given by the parameter

$$m_{th} = -\frac{\Omega^2}{4J^2}. \tag{33}$$

Of course, the above derivation is valid far from the ''fake'' transitions, Eq. (16), and under the conditions Eqs. (5) and (25).

Slopes in Fig. 5 have been obtained by a standard linear fit and then compared with the theoretical ones m_{th}, see Fig. 6.

As one can see, the agreement is very good except for small values of the Ising interaction, $J \simeq \Omega$, where the probability of near-resonant transitions becomes large, and the condition $P\epsilon \ll 1$ is not valid anymore.

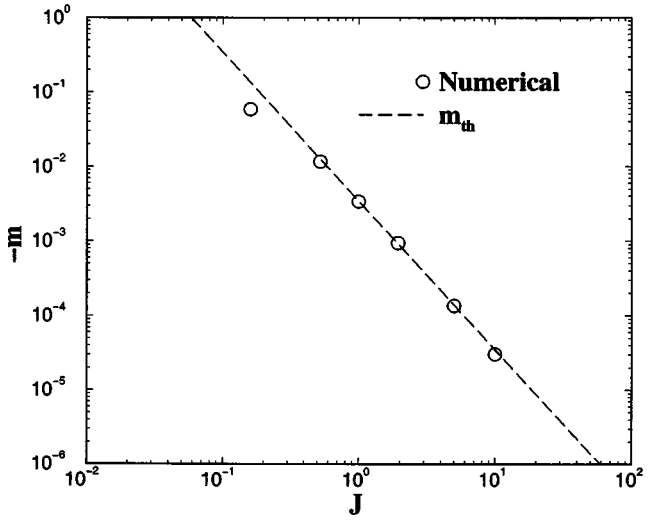

FIG. 6. Comparison between theoretical and numerical linear slopes for the fidelity, as a function of the interaction J, obtained for $\Omega = 0.118$ and $a = 100$.

Finally, let us stress that the phase correction is far from being trivial. Indeed, a different behavior of fidelity on the number of qubits is found without such phase correction.

Also note that, even under the $2\pi k$ conditions given by Eq. (26), for which $\epsilon = 0$ (so that there are no errors in modulus caused by near-resonant transitions), a phase error persists, so that, in order to improve fidelity, the same phase correction is necessary.

E. Optimal algorithm

Choosing Ω values as given by Eq. (26), one gets that the probability for near-resonant transition is zero, $\epsilon = 0$. So, only nonresonant transitions lead to unwanted states. In Fig. 7 we show the fidelity as a function of the number of spins L for $\Omega_k = 0.1216$. These data should be compared with the analogous ones indicated by triangles in Fig. 5.

As one can see, despite the closeness of these two Ω values (less than 3% of difference), the fidelity increases in two order of magnitude (see different scales on the y axis). It is clear that such preferred Ω values should be chosen in any practical implementation of the algorithm. However, due to the high instability of such resonant values, see Fig. 4, a detailed analysis can only be done within a more general study under the presence of small variations in parameters such as Ω, J, a. This study is currently in progress.

V. CONCLUSIONS

We have studied the model of a quantum computer consisting of a one-dimensional chain of 1/2 spins (qubits), placed in a time-dependent electromagnetic field. The latter is given by a sequence of rf pulses, corresponding to a chosen quantum protocol that allows to generate an entangled state for remote qubits from the initial ground state. Main attention is paid to the analysis of the dynamical fidelity,

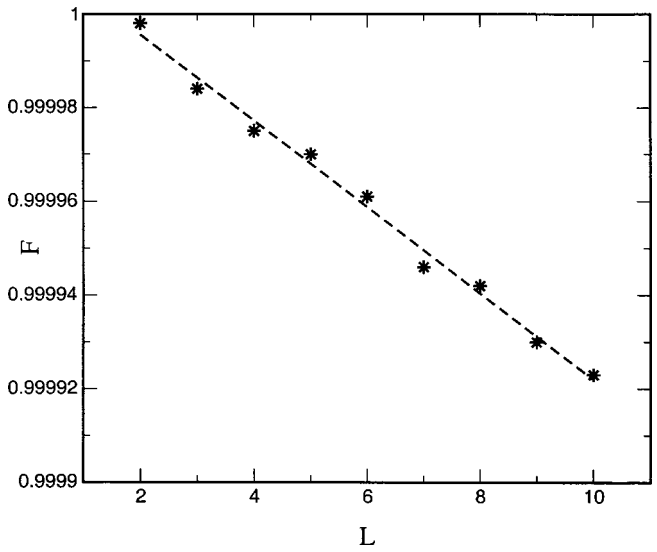

FIG. 7. The dynamical fidelity as a function of the number L of spins, for $J=1.945$ and $\Omega_k=0.1216$, $a=100$. Also shown is the best linear fit with the slope $9.2\pm0.3\times10^{-6}$.

defined as the overlap of the actual finite state with the ideal one determined by the quantum protocol.

We considered the region of the selective excitation where the resonant excitations of specific qubits can be implemented by time-dependent pulses. Analytical treatment of the stationary Hamiltonian which describes the evolution of the system during a single pulse has revealed that in the selective regime the quantum chaos cannot appear. Moreover, in this regime a perturbation theory can be applied to all quantities of interest.

Our detailed study of the dynamical fidelity manifests excellent agreement between numerical data and the predictions obtained in the perturbative approach. In particular, we have found how to choose the parameters in order to get the best dynamical fidelity for the creation of the remote entangled state. Specific attention has been paid to the dependence of the dynamical fidelity on the number L of qubits. We show, both analytically and numerically, that the dynamical fidelity decreases linearly with an increase of L, and we give an analytical estimate for the slope of this dependence.

ACKNOWLEDGMENTS

The work of GPB was supported by the Department of Energy (DOE) under the Contract No. W-7405-ENG-36, by the National Security Agency (NSA) and Advanced Research and Development Activity (ARDA). F.M.I. acknowledges the support by CONACyT (Mexico), Grant No. 34668-E. We acknowledge R. Bonifacio for useful discussions. The authors also thank the International Center at Cuernavaca for financial support during the workshop ''Chaos in few and many-body problems'' where this work was started.

[1] I.L. Chuang, R. Laflamme, P.W. Shor, and W.H. Zurek, Science **270**, 1633 (1995).
[2] V. Zelevinsky, B.A. Brown, N. Frazier, and M. Horoi, Phys. Rep. **276**, 85 (1996).
[3] T. Guhr, A. Müller-Groeling, and H.A. Weidenmüller, Phys. Rep. **299**, 189 (1999).
[4] V.K.B. Kota, Phys. Rep. **347**, 223 (2001).
[5] B. Georgeot and D.L. Shepelyansky, Phys. Rev. E **62**, 3504 (2000); **62**, 6366 (2000).
[6] G.P. Berman, F. Borgonovi, F.M. Izrailev, and V.I. Tsifrinovich, Phys. Rev. E **64**, 056226 (2001); **65**, 015204 (2001).
[7] A. Peres, Phys. Rev. A **30**, 1610 (1984); R.A. Jalabert and H.M. Pastawski, Phys. Rev. Lett. **86**, 2490 (2001); Ph. Jacquod, P.G. Silvestrov, and C.W.J. Beenakker, Phys. Rev. E **64**, 055203 (2001); N.R. Cerruti and S. Tomsovic, Phys. Rev. Lett. **88**, 054103 (2002); T. Prosen, Phys. Rev. E **65**, 036208 (2002); F.M. Cucchietti, C.H. Lewenkopf, E.R. Mucciolo, H.M. Pastawski, and R.O. Vallejos, *ibid.* **65**, 046209 (2002); G. Benenti and G. Casati, e-print quant-ph/0112132; T. Prosen and T.H. Seligman, e-print nlin.CD/;0201038; T. Prosen and M. Znidaric, J. Phys. A **34**, L681 (2001).
[8] G.P. Berman, G.D. Doolen, G.D. Holm, and V.I. Tsifrinovich, Phys. Lett. A **193**, 444 (1994).
[9] G.P. Berman, G.D. Doolen, R. Mainieri, and V.I. Tsifrinovich, *Introduction to Quantum Computers* (World Scientific, Singapore, 1998).
[10] G.P. Berman, G.D. Doolen, G.V. López, and V.I. Tsifrinovich, Phys. Rev. A **61**, 062305 (2000).
[11] G.P. Berman, G.D. Doolen, D.I. Kamenev, and V.I. Tsifrinovich, Phys. Rev. A **65**, 012321 (2002).
[12] K.J. Bruland, W.M. Dougherty, J.L. Garbini, J.A. Sidles, and S.H. Chao, Appl. Phys. Lett. **73**, 3159 (1998).
[13] D. Suter and K. Lim, Phys. Rev. A **65**, 052309 (2002).
[14] G.P. Berman, D.K. Campbell, and V.I. Tsifrinovich, Phys. Rev. B **55**, 5929 (1997).
[15] B.E. Kane, Nature (London) **393**, 133 (1998).